https://doi.org/10.48048/tis.2022.4616

First Order Mixed Mode MOS-C All-Pass Frequency Selective Analog Network with Electronic Tuning

Bhartendu Chaturvedi, Jitendra Mohan and Shiv Narain Gupta*

Department of Electronics and Communication Engineering, Jaypee Institute of Information Technology, Noida, Uttar Pradesh 201304, India

(*Corresponding author's e-mail: shivgnit@gmail.com)

Received: 9 August 2021, Revised: 9 October 2021, Accepted: 9 November 2021

Abstract

This work is intended to present a novel MOS-C design of first order frequency selective analog structure that plays essential role in phase equalization. The proposed idea employs 2 electronically tunable operational trans-conductance amplifiers, 7 MOS transistors forming active resistors and 1 grounded capacitor. Substantial flexibility to work in all 4 possible mode of operation enriches the uniqueness of proposed frequency selective structure. Non-ideal scenarios along with parasitic effects are also incorporated to explore real time performance of proposed structure. The emphasis on design has been enhanced by studying the effects of capacitor variations through Monte-Carlo analysis and the effects due to the temperature variations. Typical 0.18 μm CMOS process parameters are utilized in the verification of presented theoretical aspects through PSPICE simulation. To make room for the practicability of the proposed circuit, the experimental realization using commercially available ICs is also explored and included.

Keywords: All-pass filter, First order, Mixed mode, OTA, MOS-C

Introduction

Ever since the establishment of signal processing, analog signal processing has been recognized in the detection, measurement and process of analog signals. Consequently, various analog signal processing blocks are reported in the literature so far. Owing an extremely useful characteristic of signal selection, filters have become popular frequency selective analog block nowadays. Filter design is one of the very few areas that still has enormous scope of research. Analog filters may be classified into various categories on the basis of frequency selection properties and order of filtering. Among all possible classifications, first order all-pass filters (APFs) are gaining popularity due to their inherent attribute of phase correction. All-pass filters also work as one of the essential blocks in numerous signal processing applications such as in oscillators, communication systems, control systems, audio processing systems, healthcare equipment, etc. [1]. As a result, literature is filled with numerous all-pass filters that employ variety of active building blocks (ABBs). However, novel structures of first order all-pass frequency selective networks are still on demand [2-39]. In this paper, only those existing works are considered for study which employed operational trans-conductance amplifier (OTA) as an ABB [2-33]. All the reported first order OTA based APF can be discriminated on the basis of nature of input and output signals deciding the mode of operation. Various voltage mode (VM) APFs are documented in the existing literature [2-5,8,10,12-15,17,19,20,22-25,27,28]. Similarly, the varieties of current mode (CM) APFs [6,7,9,11,16,21,29-33] are also reported. One trans-admittance mode (TAM) APF is presented in [18]. The work presented in [26] can operate in both voltage mode and current mode simultaneously. However, none of the reported works can work in all four possible mode of operation. Furthermore, all the reported APFs are categorized as follows on the basis of several key performance parameters.

1) Passive components such as resistors and capacitors take more area during IC fabrication, thus the count of passive components should be limited. APF structures presented in [4,5,11,12,20,25,26,28,29] employ 3 or more passive components which increase circuit complexity.

2) In comparison to realizations with more than 2 active elements, filter realizations based on 1 or 2 active elements offer simpler circuit designs. APFs circuits reported in [3,7,16,19-23,25,30,33] have 3 or more than 3 active elements.

3) MOS-C filters realizations have the ability of tuning the pole frequency electronically. Filters reported in [3,7-10,13-16,18,19,21-23,27,30,33] have electronically tunable structure.

4) The use of grounded capacitor(s) is advantageous from the integrated circuits fabrication point of view. APFs with 1 or 2 grounded capacitors have been reported in [4,6,8,11-13,15,17-21,23-26,29-33].

5) The circuit's practicality is amply validated by experimental results. Practical realizations using commercially available ICs of APFs in [3-5,9,11,13,17,23] are included.

It is to be observed from the above categorizations of reported APFs that all existing circuits suffer from 1 or more limitations. With the motivation to overcome the limitations of existing OTA based analog all-pass filters, a new first order mixed mode MOS-C all-pass filter design is presented in this paper. The proposed APF employs 2 OTAs, 7 MOS transistors as active resistors and only 1 grounded capacitor as passive element. The presented structure is found more flexible since it can operate in all 4 possible operating modes namely trans-admittance mode (TAM), voltage mode (VM), current mode (CM) and trans-impedance mode (TIM). Moreover, the proposed structure also enjoys the attractive feature of electronic tunability. Furthermore, the practicability of the proposed circuit is tested by exploring commercially available ICs based experimental realization. Additionally, to confirm the superiority of the novel design, an exhaustive comparison with the most relevant existing works has been made and included in tabular form in **Table 1**.

Materials and methods

This section presents the detailed mathematical description of the proposed APF beginning with the fundamental features of the operational trans-conductance amplifier (OTA), which is used as an ABB. The proposed frequency selective structure as well as its non-ideal and parasitic investigations is given in the upcoming sub-sections.

Description of ABB: OTA

Among many of the available ABBs, one of the most popular choices is operational trans-conductance amplifier (OTA) [17,21] due to its inherent and demanded attribute of electronic tunability. **Figures 1** and **2** illustrate the symbolic representation and CMOS implementation of OTA, respectively.

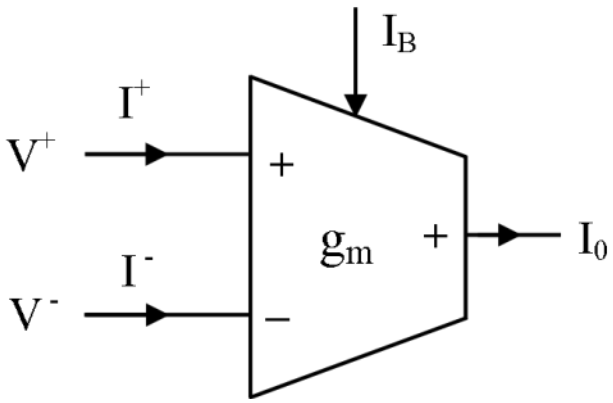

Figure 1 The symbolic representation of OTA [21].

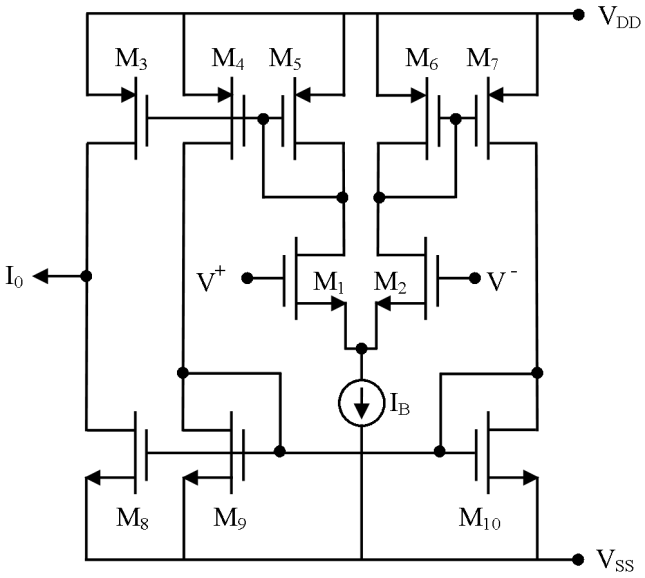

Figure 2 CMOS implementation of OTA [21].

The expressions that mathematical describe the behavior of OTA, commonly known as output current (I_0) and trans-conductance (g_m) of the device, are given in Eqs. (1) - (2), respectively.

Table 1 Comparison of the presented structure of first order all-pass frequency selective network with the most relevant OTA based existing works.

Ref.	ABB(s) Used / Count	No. of BJT / MOS transistors	Count of passive components (R+C)	Grounded capacitor(s)	Operating mode(s)	Cascadability at output	Resistorless realization	Electronic tunability	Simulation/ Experimental verification shown	THD (%)	CMOS technology (µm)	Pole frequency	Power supply (V) and Maximum power dissipation (mW)
[2]	OTA/2	–	1 + 1	No	VM	No	No	Yes	No/No	–	–	–	–
[3]	OTA/2, UGA/1	–	0 + 2	No	VM	Yes	Yes	Yes	No/Yes	–	–	1 kHz	–
[4]	OTA/1	–	4 + 1	Yes	VM	No	No	Yes	No/Yes	–	–	4.65 kHz	± 13 and –
[5]	OTA/1, OA/1	–	4 + 1	No	VM	No	No	Yes	No/Yes	–	–	20 kHz	–
[6]	OTA/2	17	1 + 1	Yes	CM	Yes	No	Yes	Yes/No	–	0.80	100 kHz	± 5 and 138
[7]	OTA/2, OA/2	32	0 + 0	NA	CM	Yes	Yes	Yes	Yes/No	–	1.2	1 MHz	± 2.5 and –
[8]	OTA/1, UGDA/1	22	0 + 1	Yes	VM	Yes	Yes	Yes	Yes/No	0.3	0.35	–	± 2.5 and –
[9]	OTA/1	12	0 + 1	No	CM	Yes	Yes	Yes	No/Yes	0.8	–	1.32 MHz	± 2.5 and –
[10]	OTA/1, UVC/1	–	0 + 1	No	VM	No	Yes	Yes	Yes/No	–	–	1 MHz	± 2 and –
[11]	OTA/2	–	2 + 1	Yes	CM	Yes	No	Yes	No/Yes	–	–	–	–
[12]	OTA/1, DVCC/1	25	2 + 1	Yes	VM	Yes	No	Yes	Yes/No	2	0.50	100 kHz	± 1.85 and –
[13]	OTA/1, DIBA/1	–	0 + 1	Yes	VM	No	Yes	Yes	No/Yes	0.1-1	–	318 kHz	± 5 and –
[14]	OTA/1	14	0 + 1	No	VM	Yes	Yes	Yes	Yes/No	2	0.35	1 MHz	± 1.5 and –
[15]	OTA/1	24	0 + 1	Yes	VM	Yes	Yes	Yes	Yes/No	2	0.35	1 MHz	+1.5 and –
[16]	OTA/2, OA/1	30	0 + 0	NA	CM	No	Yes	Yes	Yes/No	0.58	0.25	2.06 MHz	± 2 and –
[17]	OTA/2	16	1 + 1	Yes	VM	Yes	No	Yes	No/Yes	–	0.18	8.05 kHz	±0.4/±5 and 0.0472/9
[18]	OTA/2	22	0 + 1	Yes	TAM	Yes	Yes	Yes	Yes/No	1.21-2.83	0.18	1.53 kHz	± 0.85 and 4.76

Ref.	ABB(s) Used / Count	No. of BJT / MOS transistors	Count of passive components (R+C)	Grounded capacitor(s)	Operating mode(s)	Cascadability at output	Resistorless realization	Electronic tunability	Simulation/ Experimental verification shown	THD (%)	CMOS technology (µm)	Pole frequency	Power supply (V) and Maximum power dissipation (mW)
[19]	OTA/3	12	0 + 1	Yes	VM	No	Yes	Yes	Yes/No	–	0.50	246.75 kHz	± 3 and –
[20]	OTA/6, OA/1	–	2 + 1	Yes	VM	No	No	Yes	Yes/No	–	–	20 kHz	–
[21]	OTA/3	36	0 + 1	Yes	CM	Yes	Yes	Yes	Yes/No	–	0.50	1 MHz	± 1.8 and 2.49
[22]	OTA/3	12	0 + 1	No	VM	No	Yes	Yes	Yes/No	–	0.35	2.89 MHz	± 1.65 and –
[23]	OTA/2, ECCII/1	–	0 + 1	Yes	VM	Yes	Yes	Yes	No/Yes	–	–	150 kHz	± 5 and –
[24]	OTA/2	–	1 + 1	Yes$	VM	No	No	Yes	Yes/No	–	–	–	–
[25]	CF/I/1, CA/1, OTA/1	–	2 + 1	Yes	VM	Yes	No	Yes	Yes/No	–	–	–	–
[26]	OTA/2	24	4 + 1	Yes	VM, CM	No	No	Yes	Yes/No	–	0.18	953.5 kHz	± 1 and –
[27]	OTA/2	24	0 + 1	No	VM	No	Yes	Yes	Yes/No	–	0.18	1 kHz	± 1.8 and –
[28]	OTA/1	08	1 + 2	No	VM	Yes	No	Yes	Yes/No	–	0.18	–	± 2 and –
[29]	OTA/1	12	2 + 1	Yes	CM	Yes	No	Yes	Yes/No	–	0.50	15.9 kHz	± 1.5 and –
[30]	OTA/3	36	0 + 1	Yes	CM	Yes	Yes	Yes	Yes/No	0.64	0.25	7 MHz	± 1.5 and –
[31]	OTA/1	12	1 + 1	Yes	CM	Yes	No	Yes	Yes/No	–	0.50	1 MHz	± 2 and –
[32]	OTA/1	12	1 + 1	Yes	CM	Yes	No	Yes	Yes/No	–	0.50	1 MHz	± 2 and –
[33]	OTA/3	63	0 + 1	Yes	CM	Yes	Yes	Yes	Yes/No	–	–	0.15 MHz	± 2.5 and –
Proposed	**OTA/2**	**27**	**0 + 1**	**Yes**	**VM, TAM, CM, TIM**	**Yes#**	**Yes**	**Yes**	**Yes/Yes**	**0.186**	**0.18**	**1.561 MHz**	**± 1** and **0.717**

Abbreviations: ABB: Active building block, OTA: Operational trans-conductance amplifier, UGA: Unity gain amplifier, OA: Operational amplifier, UGDA: Unity gain differential amplifier, UVC: Universal voltage conveyor, DVCC: Differential voltage current conveyor, DIBA: Differential-input buffered amplifier, ECCII: Electronically tunable second generation current conveyor, CF/I: Current follower/inverter, CA: Current amplifier, BJT: Bipolar junction transistor, MOS: Metal oxide semiconductor, R: Resistor, C: Capacitor, VM: Voltage mode, TAM: Trans-admittance mode, CM: Current mode, TIM: Trans-impedance mode, THD: Total harmonic distortion, NA: Not applicable, –: Not available, $: Grounded capacitor is utilized in 3 out of 6 presented structures, #: This feature is available in CM and TAM.

$$I_0 = g_m(V^+ - V^-) \tag{1}$$

$$g_m = \sqrt{\mu_n C_{ox} \frac{W}{L} I_B} \tag{2}$$

where, I_B is bias current; W/L is transistor aspect ratio; C_{ox} is gate oxide capacitance per unit area; μ_n is mobility of electrons; V^+ and V^- are the voltages at non-inverting and inverting input terminals of OTA, respectively.

Proposed circuit

The proposed mixed mode MOS-C first order APF is shown in **Figure 3**. It employs 2 OTAs, 7 NMOS transistors as active resistors and a grounded capacitor. The transistor M_{R1} realizes a floating active resistor R_{M1} [40] and 3 grounded active resistors $R_{M2,}$ R_{M3} and R_{M4} [41], are realized using NMOS pairs M_{R2}-$M_{R2'}$, M_{R3}-$M_{R3'}$ and M_{R4}-$M_{R4'}$, respectively. The mathematical expressions representing floating and grounded resistors are given in Eqs. (3) - (4), respectively.

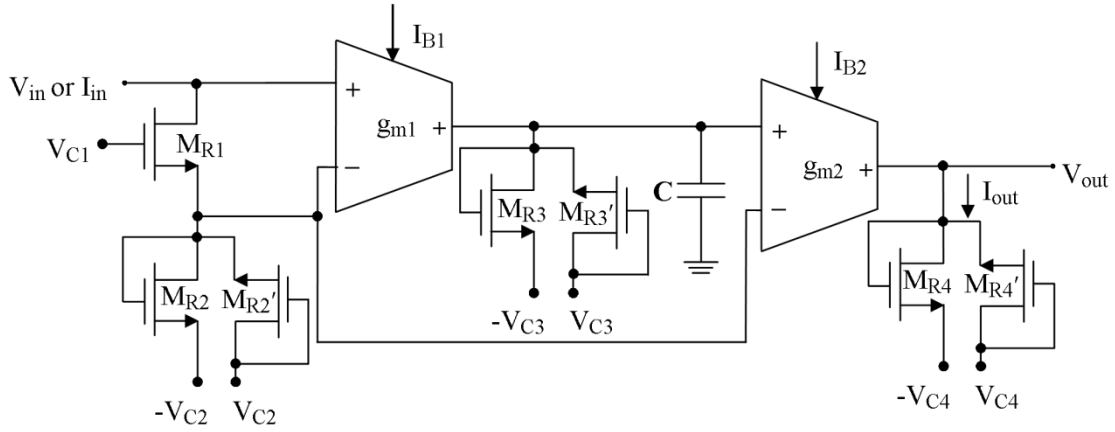

Figure 3 Proposed mixed mode MOS-C first order APF.

$$R_{M1} = \left[\mu_n C_{ox} \left(\frac{W}{L} \right) \left(V_{C1} - V_T \right) \right]^{-1} \tag{3}$$

$$R_{Mj} = \left[2\mu_n C_{ox} \left(\frac{W}{L} \right) \left(V_{Cj} - V_T \right) \right]^{-1} \tag{4}$$

where, j = 2, 3 and 4, C_{ox}, μ_n, W/L are the physical parameters of MOS transistors, V_T is the threshold voltage and V_{C1}, V_{C2}, V_{C3} and V_{C4} are the control voltages.

It is to be emphasized that the proposed configuration can operate in all 4 possible modes of operations (TAM, VM, CM and TIM). The working process of all 4 possible modes is explained in following 2 cases.

Case-I Working process in TAM and VM

In TAM and VM, the required input should be voltage signal. Therefore, input voltage (V_{in}) as shown in **Figure 3** is considered as input signal. However, the available output signal should be current (I_{out}) in case of TAM and should be voltage (V_{out}) in case of VM. Consequently, the mathematical expressions for output current (I_{out}) and output voltage (V_{out}) for TAM and VM, are given in Eqs. (5) - (6), respectively.

$$I_{out} = g_{m2} \left[g_{m1} \left(V_{in} - \frac{V_{in} R_{M2}}{R_{M1} + R_{M2}} \right) \frac{R_{M3}}{(1 + sR_{M3}C)} - \frac{V_{in} R_{M2}}{R_{M1} + R_{M2}} \right] \tag{5}$$

$$V_{out} = I_{out} R_{M4} = R_{M4} g_{m2} \left[g_{m1} \left(V_{in} - \frac{V_{in} R_{M2}}{R_{M1} + R_{M2}} \right) \frac{R_{M3}}{(1 + sR_{M3}C)} - \frac{V_{in} R_{M2}}{R_{M1} + R_{M2}} \right] \tag{6}$$

Here, g_{m1} and g_{m2} are the trans-conductances of first and second OTA, respectively.

Eqs. (5) - (6) can be further simplified to get the transfer functions of APF in TAM and VM, by considering $R_{M1} = R_{M2} = R_M/2$, $R_{M3} = R_{M4} = R_M$, $g_{m1} = g_{m2} = g_m$ and $g_m R_M = 2$. The simplified transfer functions are given in Eqs. (7) - (8).

$$T_{AP(TAM)}(s) = \frac{I_{out}(s)}{V_{in}(s)} = \frac{1}{R_M} . \left[\frac{1 - sR_M C}{1 + sR_M C} \right] \tag{7}$$

$$T_{AP(VM)}(s) = \frac{V_{out}(s)}{V_{in}(s)} = \left[\frac{1 - sR_M C}{1 + sR_M C} \right] \tag{8}$$

Eqs. (7) - (8) are in the coherence with the standard transfer function of first order all-pass filter.

Case-II Working process in CM and TIM

The required input should be current signal in CM and TIM. Therefore, input current (I_{in}) as shown in **Figure 3** is considered as input signal in this case. However, the available output signal should be current (I_{out}) in case of CM and should be voltage (V_{out}) in case of TIM. The mathematical expressions for output current (I_{out}) and output voltage (V_{out}) for CM and TIM are given in Eqs. (9) - (10), respectively.

$$I_{out} = g_{m2}\left[g_{m1}\left(I_{in}\left(R_{M1} + R_{M2} \right) - I_{in} R_{M2} \right) \frac{R_{M3}}{(1 + sR_{M3}C)} - I_{in} R_{M2} \right] \tag{9}$$

$$V_{out} = R_{M4} I_{out} = R_{M4} g_{m2}\left[g_{m1}\left(I_{in}\left(R_{M1} + R_{M2} \right) - I_{in} R_{M2} \right) \frac{R_{M3}}{(1 + sR_{M3}C)} - I_{in} R_{M2} \right] \tag{10}$$

By analyzing (9) and (10) and via considering $R_{M1} = R_{M2} = R_M/2$, $R_{M3} = R_{M4} = R_M$, $g_{m1} = g_{m2} = g_m$ and $g_m R_M = 2$, the transfer functions of APF in CM and TIM are given in Eqs. (11) - (12), respectively.

$$T_{AP(CM)}(s) = \frac{I_{out}(s)}{I_{in}(s)} = \left[\frac{1 - sR_M C}{1 + sR_M C} \right] \tag{11}$$

$$T_{AP(TIM)}(s) = \frac{V_{out}(s)}{I_{in}(s)} = R_M \left[\frac{1 - sR_M C}{1 + sR_M C} \right] \tag{12}$$

The magnitude and phase expressions are given below.

$$\left| T_{AP(TAM)} \right| = \frac{1}{R_M},\ \left| T_{AP(VM)} \right| = \left| T_{AP(CM)} \right| = 1,\ \left| T_{AP(TIM)} \right| = R_M \tag{13}$$

$$\phi_{AP}(\omega) = -2\tan^{-1}\left[\omega R_M C \right] = -2\tan^{-1}\left[\frac{2\omega C}{g_m} \right] \tag{14}$$

The pole frequency and sensitivity figures with respect to active and passive components are given in Eqs. (15) - (16), respectively.

$$f_0 = \frac{1}{2\pi R_M C} = \frac{g_m}{4\pi C} \tag{15}$$

$$S_{g_m}^{f_0} = -S_C^{f_0} = -S_{R_M}^{f_0} = 1 \tag{16}$$

From Eq. (16), it can be observed that the presented circuit has good sensitivity figures. It is also observed from the Eqs. (7), (8), (11) and (12) that the presented structure can operate in all possible 4 modes. It is also worth mentioned and confirmed from Eqs. (14) - (15) that the phase response and pole frequency of the presented APF circuit is electronically tunable with the trans-conductance (g_m), which value can be further controlled with the help of bias current, I_B. Therefore, the presented circuit is enabled with the significant attribute of electronic tunability.

Non-ideal analysis

In the previous sub-section, the ideal behavioral model of the active device is considered for analyzing the proposed circuit of first order mixed mode MOS-C APF. However, non-ideal properties of OTA may also affect the performance of the proposed circuit. Firstly, the non-ideal factor of the trans-conductance is considered which transforms the input voltage into an output current. By considering this non-ideal factor of trans-conductance, the output current of non-ideal OTA is modified as follows:

$$I_{oi} = \pm\beta_i g_{mi}(V^+ - V^-) \tag{17}$$

where, g_{mi} (i = 1, 2) is the trans-conductance of i^{th} OTA and β_i (i = 1, 2) is the inaccurate trans-conductance factor of i^{th} OTA. The proposed circuit of **Figure 3** is reanalyzed using Eq. (17), the non-ideal transfer functions of the proposed circuit are expressed in Eqs. (18) - (21).

$$T_{AP(VM)}(s) = \frac{V_{out}(s)}{V_{in}(s)} = \beta_2 g_{m2} R_{M4}\left[\frac{\beta_1 g_{m1} R_{M3}}{1+sR_{M3}C}\left(\frac{R_{M1}}{R_{M1}+R_{M2}}\right) - \frac{R_{M2}}{R_{M1}+R_{M2}}\right] \tag{18}$$

$$T_{AP(TAM)}(s) = \frac{I_{out}(s)}{V_{in}(s)} = \beta_2 g_{m2}\left[\frac{\beta_1 g_{m1} R_{M3}}{1+sR_{M3}C}\left(\frac{R_{M1}}{R_{M1}+R_{M2}}\right) - \frac{R_{M2}}{R_{M1}+R_{M2}}\right] \tag{19}$$

$$T_{AP(CM)}(s) = \frac{I_{out}(s)}{I_{in}(s)} = \beta_2 g_{m2}\left[\frac{\beta_1 g_{m1} R_{M1} R_{M3}}{1+sR_{M3}C} - R_{M2}\right] \tag{20}$$

$$T_{AP(TIM)}(s) = \frac{V_{out}(s)}{I_{in}(s)} = \beta_2 g_{m2} R_{M4}\left[\frac{\beta_1 g_{m1} R_{M1} R_{M3}}{1+sR_{M3}C} - R_{M2}\right] \tag{21}$$

By analyzing Eqs. (18) - (21), if $R_{M1} = R_{M2} = R_M/2$, $R_{M3} = R_{M4} = R_M$, $g_{m1} = g_{m2} = g_m$ and $g_m R_M = 2$, the non-ideal transfer functions of the proposed APF are given in Eqs. (22) - (25).

$$T_{AP(VM)}(s) = \frac{V_{out}(s)}{V_{in}(s)} = \beta_2\left[\frac{\beta_1 g_m R_M - 1 + sR_M C}{1+sR_M C}\right] \tag{22}$$

$$T_{AP(TAM)}(s) = \frac{I_{out}(s)}{V_{in}(s)} = \frac{\beta_2}{R_M}\left[\frac{\beta_1 g_m R_M - 1 + sR_M C}{1+sR_M C}\right] \tag{23}$$

$$T_{AP(CM)}(s) = \frac{I_{out}(s)}{I_{in}(s)} = \beta_2\left[\frac{\beta_1 g_m R_M - 1 + sR_M C}{1+sR_M C}\right] \tag{24}$$

$$T_{AP(TIM)}(s) = \frac{V_{out}(s)}{I_{in}(s)} = \beta_2 R_M\left[\frac{\beta_1 g_m R_M - 1 + sR_M C}{1+sR_M C}\right] \tag{25}$$

The non-ideal expressions of magnitude, phase and pole frequency (f_o) of presented APF are given below.

$$\left|T_{AP(VM)}\right| = \left|T_{AP(CM)}\right| = \sqrt{\frac{\left[\beta_2(2\beta_1-1)\right]^2 + \left[\beta_2 R_M C\right]^2}{1+\left[R_M C\right]^2}} \tag{26}$$

$$\left|T_{AP(TAM)}\right| = \frac{1}{R_M}\sqrt{\frac{\left[\beta_2(2\beta_1-1)\right]^2 + \left[\beta_2 R_M C\right]^2}{1+\left[R_M C\right]^2}} \tag{27}$$

$$\left|T_{AP(TIM)}\right| = R_M\sqrt{\frac{\left[\beta_2(2\beta_1-1)\right]^2 + \left[\beta_2 R_M C\right]^2}{1+\left[R_M C\right]^2}} \tag{28}$$

$$\phi_{AP}(\omega) = -\tan^{-1}\left(\frac{\omega R_M C}{2\beta_1 - 1}\right) - \tan^{-1}\left(\omega R_M C\right) \tag{29}$$

$$f_0 = \frac{1}{2\pi R_M C} = \frac{g_m}{4\pi C} \tag{30}$$

It is evident from Eq. (30) that the pole frequency is unaltered and found same as Eq. (15). It is also observed that the performance of the proposed mixed mode MOS-C all-pass filter is less affected by the trans-conductance non-ideal factors β_1 and β_2.

Parasitic analysis

To anticipate the effects of parasitic on the proposed circuit, the parasitic model of OTA [17] is used. **Figure 4** illustrates the structure of the OTA, which includes parasitic. The parasitic resistors and capacitors looking at the non-inverting (V^+) and inverting (V^-) terminals of the OTA are R_{V+}, C_{V+}, R_{V-} and C_{V-}, respectively. The parasitic resistors and capacitors that appear at the output terminal, V_{out}, are the R_o and C_o. Taking all the parasitic into consideration along with $R_{M1} = R_{M2} = R_M/2$, $R_{M3} = R_{M4} = R_M$, $g_{m1} = g_{m2} = g_m$, $g_mR_M = 2$ and by using Eq. (1), the proposed APF is reanalyzed. The modified transfer functions are given in Eqs. (31) - (34).

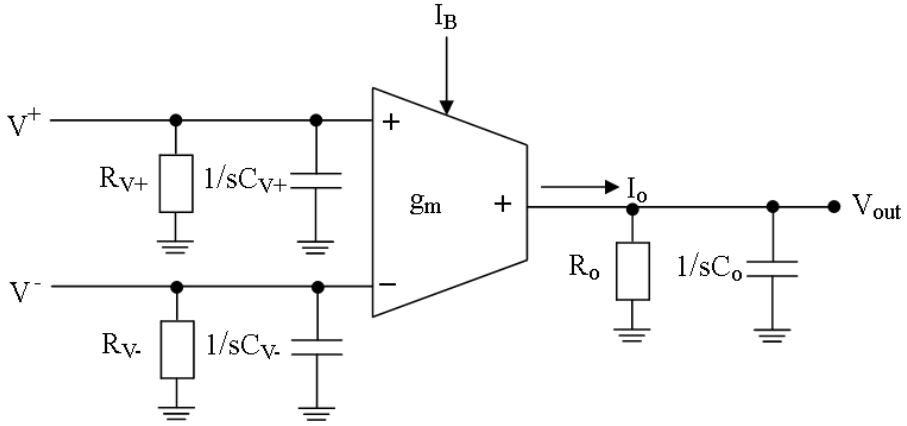

Figure 4 The OTA model with parasitic [17].

$$T_{AP(VM)}(s) = \frac{V_{out}(s)}{V_{in}(s)} = \frac{s(C_{T2} - C_{T3}) + \left(G_{T2} - G_{T3} + \frac{1}{R_M}\right)}{\frac{R_M^2}{4}\left(sC_{T2} + G_{T2} + \frac{4}{R_M}\right)\left(sC_{T3} + G_{T3} + \frac{1}{R_M}\right)\left(sC_{T4} + G_{T4} + \frac{1}{R_M}\right)} \tag{31}$$

$$T_{AP(TAM)}(s) = \frac{I_{out}(s)}{V_{in}(s)} = \frac{1}{R_M}\left(\frac{s(C_{T2} - C_{T3}) + \left(G_{T2} - G_{T3} + \frac{1}{R_M}\right)}{\frac{R_M}{4}\left(sC_{T2} + G_{T2} + \frac{4}{R_M}\right)\left(sC_{T3} + G_{T3} + \frac{1}{R_M}\right)}\right) \tag{32}$$

$$T_{AP(CM)}(s) = \frac{I_{out}(s)}{I_{in}(s)} = \frac{2}{R_M}\left(\frac{s(C_{T2} - C_{T3}) + \left(G_{T2} - G_{T3} + \frac{1}{R_M}\right)}{\left(sC_{T3} + G_{T3} + \frac{1}{R_M}\right).\left[\frac{R_M}{2}\left(sC_{T2} + G_{T2} + \frac{4}{R_M}\right)\left(sC_{T1} + G_{T1}\right) + \left(sC_{T2} + G_{T2} + \frac{2}{R_M}\right)\right]}\right) \tag{33}$$

$$T_{AP(TIM)}(s) = \frac{V_{out}(s)}{I_{in}(s)} = \frac{2}{R_M}\left(\frac{s(C_{T2} - C_{T3}) + \left(G_{T2} - G_{T3} + \frac{1}{R_M}\right)}{\left(sC_{T3} + G_{T3} + \frac{1}{R_M}\right)\left(sC_{T4} + G_{T4} + \frac{1}{R}\right).\left[\frac{R}{2}\left(sC_{T2} + G_{T2} + \frac{4}{R_M}\right)\left(sC_{T1} + G_{T1}\right) + \left(sC_{T2} + G_{T2} + \frac{2}{R_M}\right)\right]}\right) \tag{34}$$

where, $G_{T2} = G_{V1-} + G_{V2-}$, $C_{T2} = C_{V1-} + C_{V2-}$, $G_{T3} = G_{O1} + G_{V2+}$, $C_{T3} = C_{O1} + C_{V2+} + C$, $G_{T4} = G_{O2}$, $C_{T4} = C_{O2}$, $G_{V1-}=1/R_{V1-}$, $G_{V2-}=1/R_{V2-}$, $G_{O1}=1/R_{O1}$, $G_{O2}=1/R_{O2}$. R_{V1-}, C_{V1-}, R_{V2-}, C_{V2-} and R_{V1+}, C_{V1+}, R_{V2+}, C_{V2+} are the parasitic resistors and capacitors looking at inverting (V^-) and non-inverting (V^+) terminals of the first and second OTA, respectively. $R_{O1,}$ C_{O1} and $R_{O2,}$ C_{O2} are the parasitic resistors and capacitors at outputs of first and second OTA, respectively. From Eqs. (31) - (34), it can be concluded that for large value of external active resistors and capacitor as compared to parasitic resistors and capacitors, the proposed filter works well under the influence of the device parasitic. The simulated values of various parasitic of the

OTA are listed in **Table 2**. In addition, the OTA has −3 dB bandwidth of 195.123 MHz and dynamic input voltage range of 100 to −100 mV.

Table 2 Simulated values of various parasitic of the OTA.

Various parasitic at different terminals	Simulated values
Parasitic at V^+ Terminal (R_{V+}, C_{V+})	1×10^{20} Ω, 2.74 fF
Parasitic at V^- Terminal (R_{V-}, C_{V-})	1×10^{20} Ω, 2.73 fF
Parasitic at I_0 Terminal (R_0, C_0)	3.564×10^5 Ω, 3.18 fF

Results and discussion

To validate the performance characteristics of the proposed first order mixed mode MOS-C APF, simulations using PSPICE with 180 nm CMOS process parameters are done. In the simulation, a CMOS realization of OTA as shown in **Figure 2** is used with ±1 V power supply voltages. **Table 3** shows the aspect ratios of MOS transistors. The APF is designed at the pole frequency (f_o) of 1.561 MHz. To achieve $2R_{M1} = 2R_{M2} = R_{M3} = R_{M4} = R_M$ =10.2 kΩ, the gate control voltages are set to V_{C1} = 0.7191 V with W/L ratios of 0.36/0.18 µm for floating active resistor R_{M1} and V_{C2} = 0.4827 V, $V_{C3} = V_{C4}$ = 0.4508 V with W/L ratios of 4.5 µm /0.18 µm for realizing three grounded active resistors R_{M2}, R_{M3} and R_{M4}. In addition, capacitor of 10 pF is considered in simulation. In order to provide the value of trans-conductance as 196 µA/V, the biasing current is chosen as 52.23 µA. **Figures 5 - 8** demonstrate the phase and gain responses of the presented circuit in TAM, VM, CM and TIM, respectively.

Table 3 Aspect ratios of the transistors.

MOSFETS	Width (µm)	Length (µm)
M1, M2	5.67	0.72
M3, M4, M5, M6, M7	2.16	0.72
M8, M9, M10	1.44	0.72

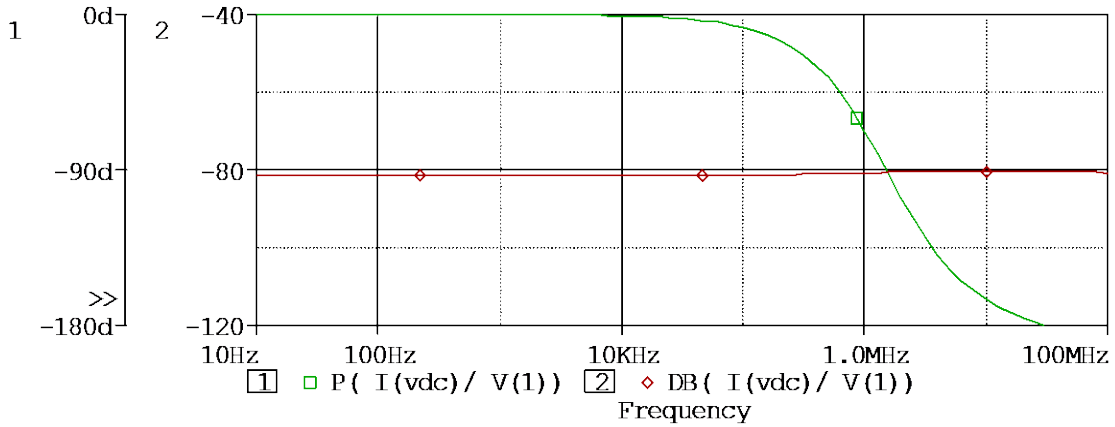

Figure 5 Simulated gain and phase responses of proposed APF in TAM.

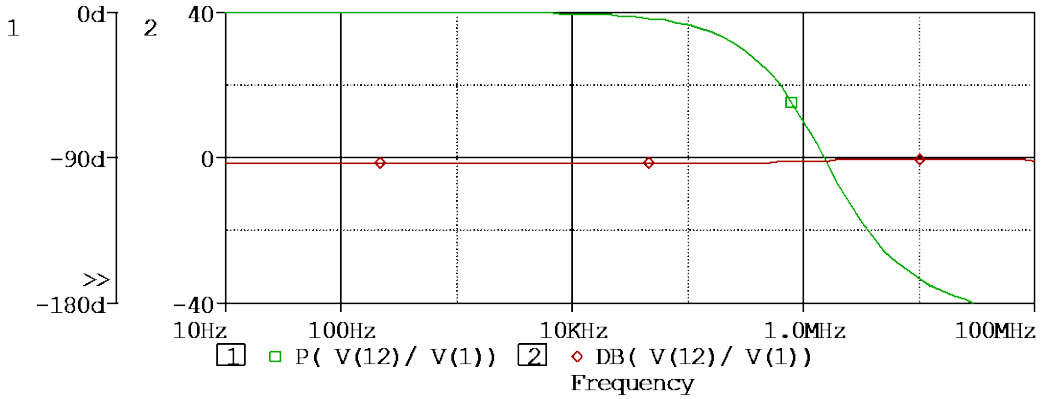

Figure 6 Simulated gain and phase responses of proposed APF in VM.

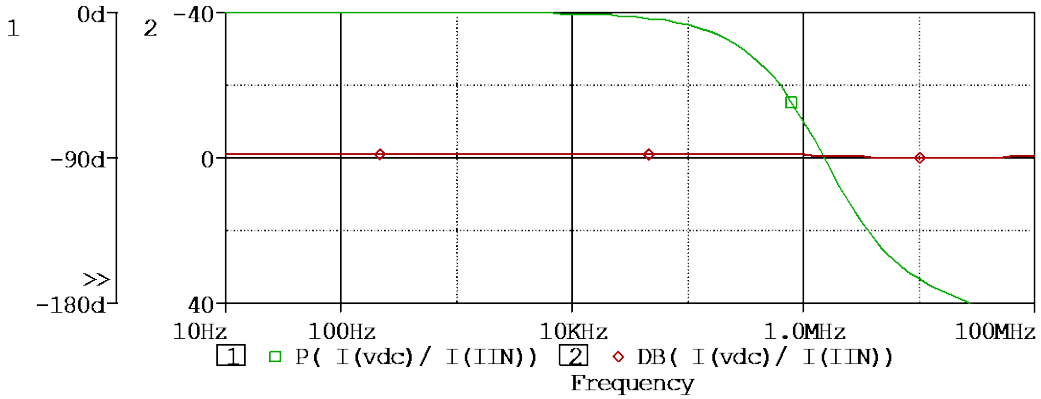

Figure 7 Simulated gain and phase responses of proposed APF in CM.

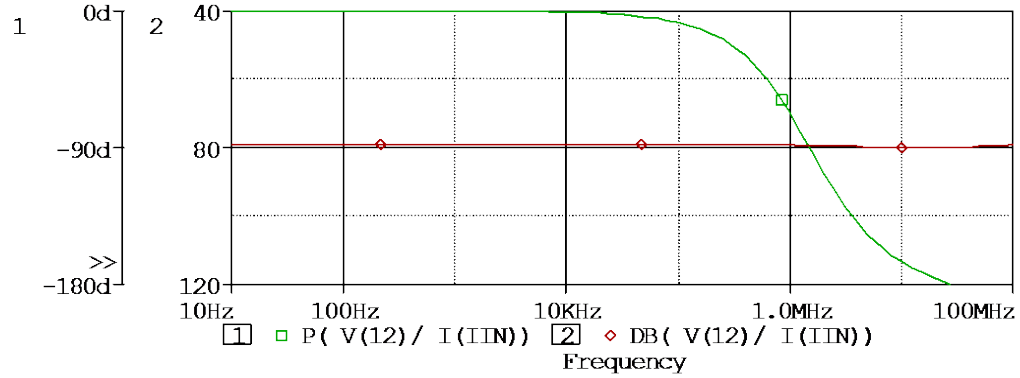

Figure 8 Simulated gain and phase responses of proposed APF in TIM.

The simulated frequency is 1.505 MHz with only 3.72 % inaccuracy. The difference between theoretical and simulated pole frequency is quite small and within an acceptable range. The dissipated power of proposed structure is found as 0.717 mW only. The gain and phase responses of the APF structure in TAM, VM, CM and TIM are tuned at 1.072, 1.286 and 1.505 MHz by setting the bias currents to $I_{B1} = I_{B2} = I_B$ as 25, 34 and 52.23 µA, respectively are shown in **Figures 9 - 12**, respectively. These variations in pole frequency further confirm that the pole frequency (f_o) can be electronically tuned easily with a fine variation in bias current (I_B).

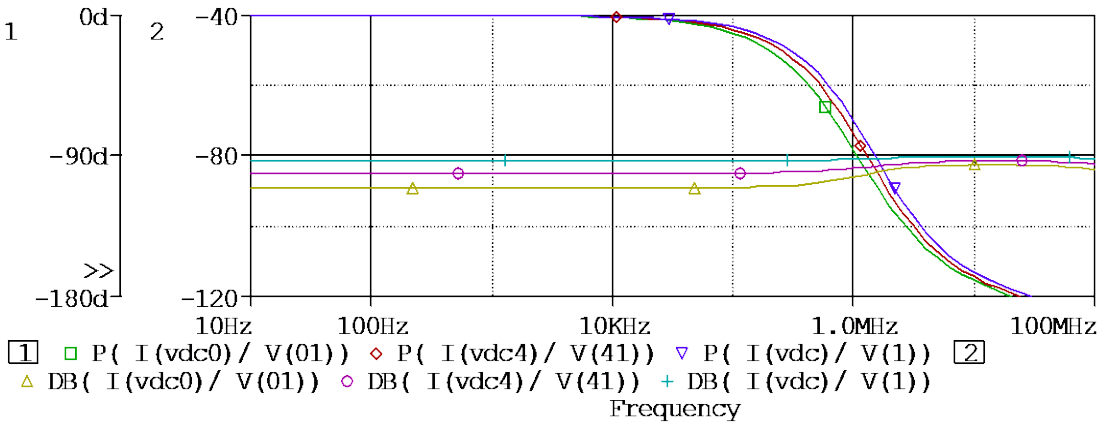

Figure 9 Gain and phase responses of proposed APF in TAM at different bias current (I_B).

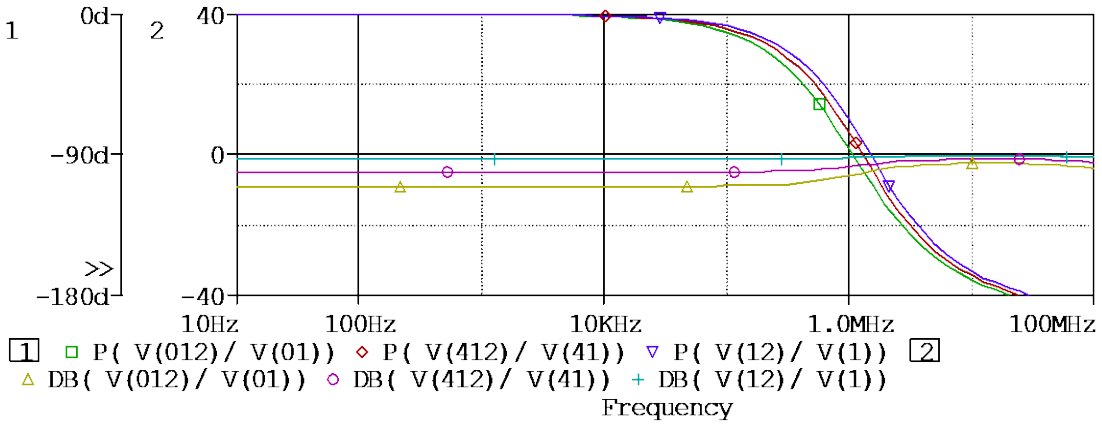

Figure 10 Gain and phase responses of proposed APF in VM at different bias current (I_B).

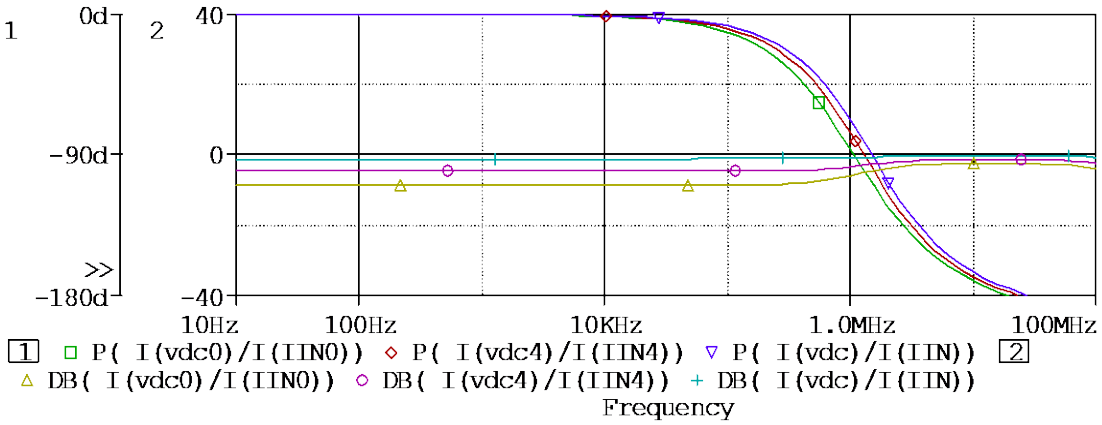

Figure 11 Gain and phase responses of proposed APF in CM at different bias current (I_B).

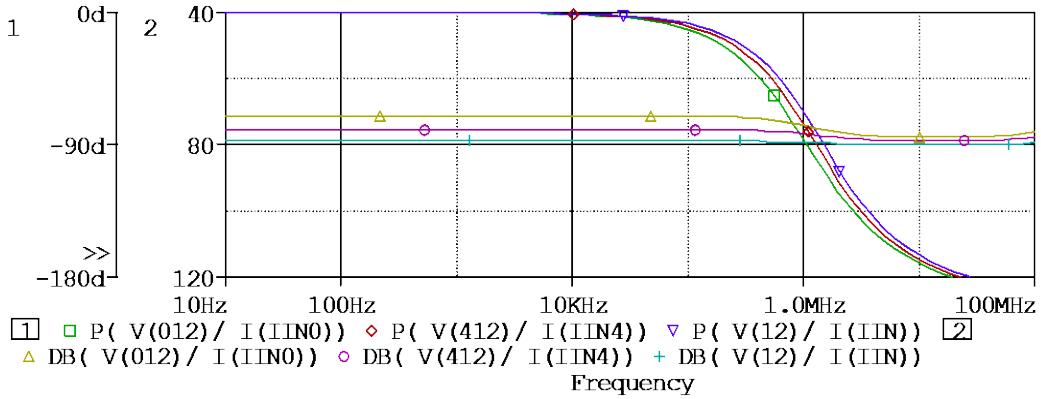

Figure 12 Gain and phase responses of proposed APF in TIM at different bias current (I_B).

Figures 13 and **14** show the time domain waveforms of input and output for VM and CM responses, respectively. At pole frequency, there is a 90 ° phase shift between the input and output for VM and CM responses, respectively. **Figures 15** and **16** demonstrate the Lissajous patterns for VM and CM responses, respectively. The circle in **Figures 15** and **16** indicates that the input and output signals are 90 ° out of phase. The real time performance of the proposed circuit through Monte-Carlo (MC) analysis is also evaluated while considering 100 runs variations in capacitor. The histograms of **Figures 17** and **18** demonstrate the MC simulation results with a 15 % Gaussian deviations in capacitor value for TAM and VM responses, respectively. According to the simulations, for VM APF, the f_0 value of the filter is affected in the range of –1.1 to +1.5 %, with a mean value of 1.519 MHz and a standard deviation of 8.256 kHz. As a consequence of the analysis results, it is evident that the presented first order APF has great sensitivity. The proposed circuit's thermal performance is also examined. **Figure 19** shows that as the temperature rises from 25 - 115 °C with step size of 10 °C, the pole frequency decreases from 1.51 - 1.17 MHz. This change is within acceptable range, indicating that the circuit has excellent thermal performance. Electronically tunability is another important fundamental feature that has become significantly important in terms of managing performance parameters. **Figure 20** validates the feature of electronic tuning of pole frequency with bias current (I_B) variation in the range of 20 - 70 µA.

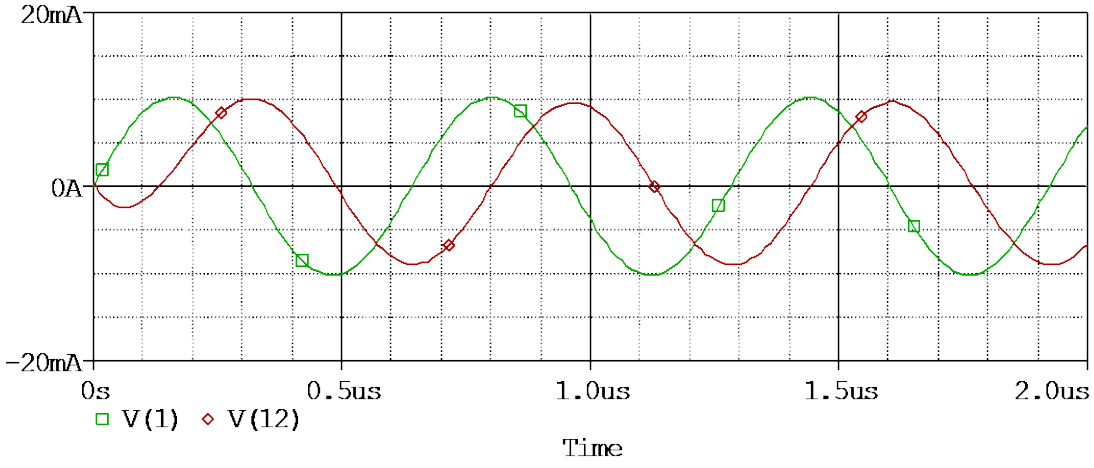

Figure 13 Time domain waveforms of input and output for VM response at pole frequency.

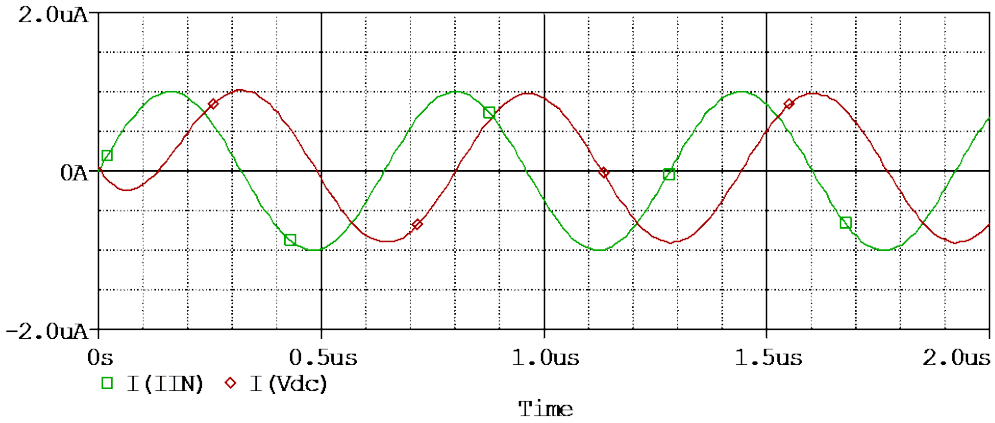

Figure 14 Time domain waveforms of input and output for CM response at pole frequency.

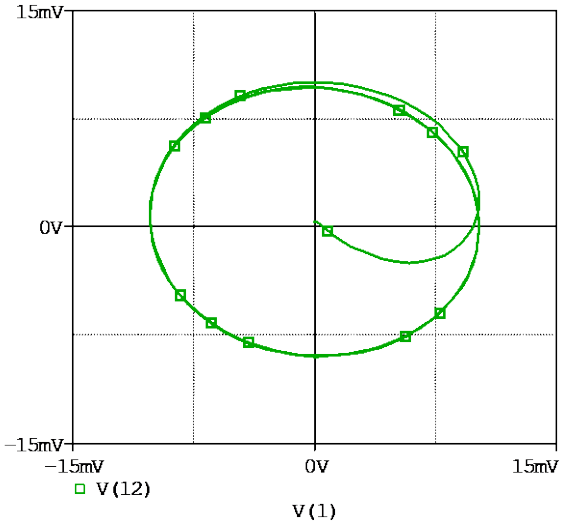

Figure 15 Lissajous pattern for VM response (V_{in} vs V_{out}).

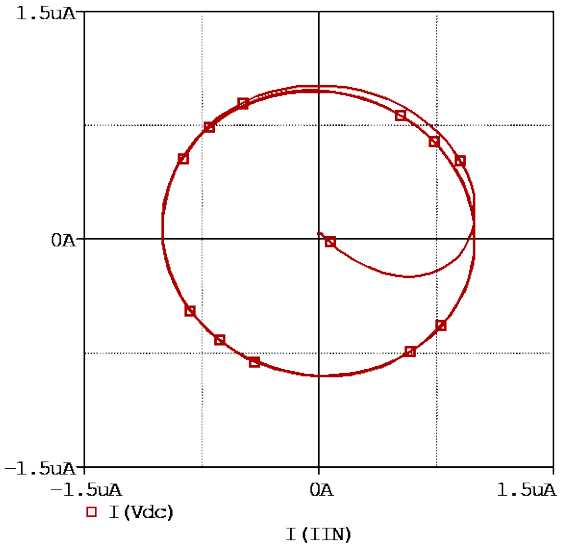

Figure 16 Lissajous pattern for CM response (I_{in} vs I_{out}).

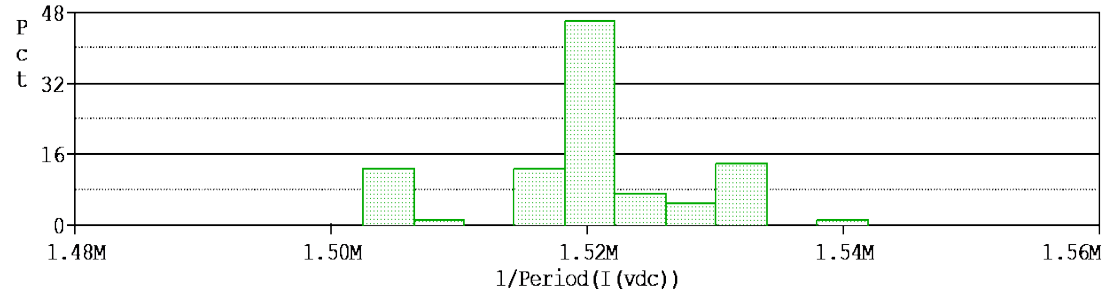

Figure 17 MC simulations for TAM response with 15 % deviations in capacitor value.

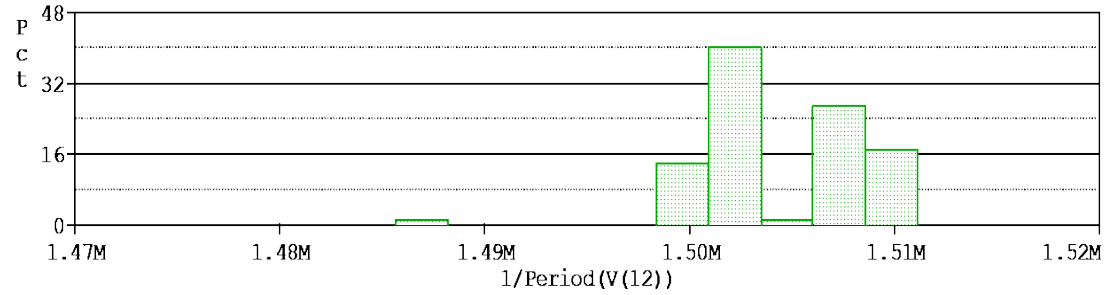

Figure 18 MC simulations for VM response with 15 % deviations in capacitor value.

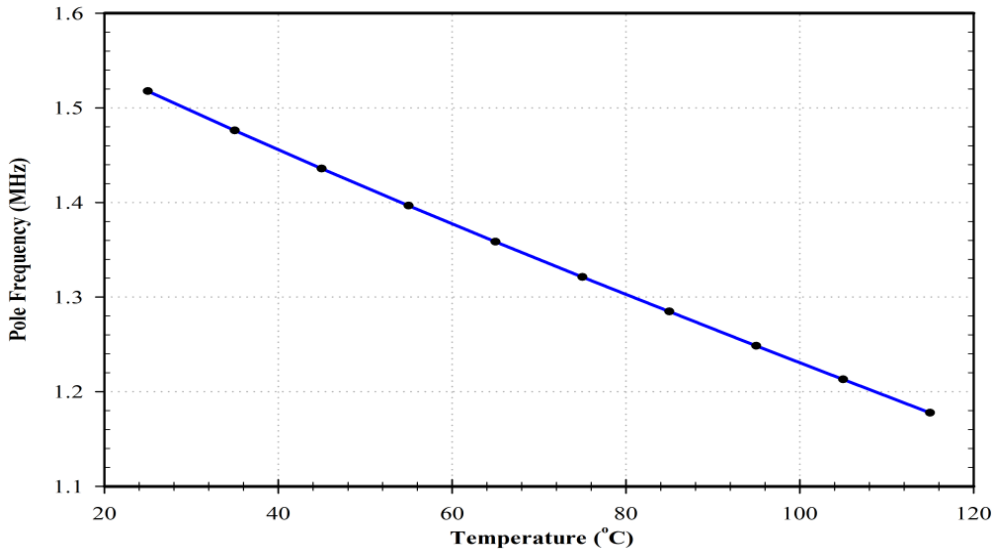

Figure 19 Pole frequency variations with temperature in the range of 25 - 115 °C.

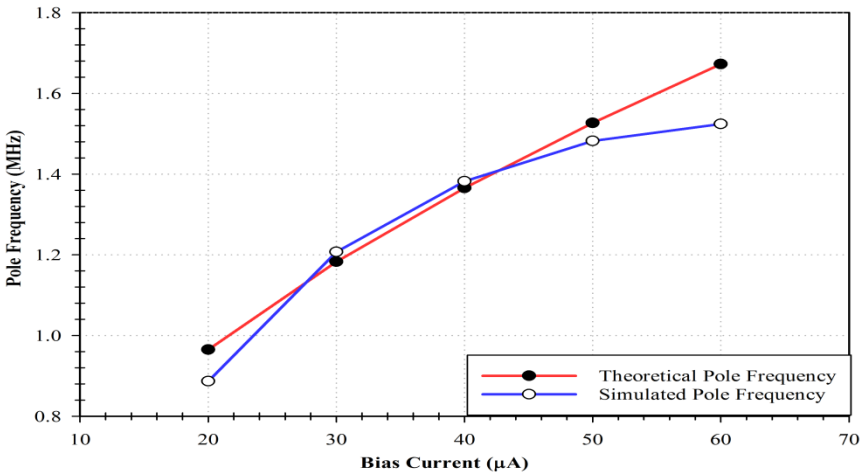

Figure 20 Pole frequency variations with bias current variation in the range of 20 - 70 µA.

Experimental verification

The possible realizations using commercially available ICs extend the practicability and feasibility aspects of novel ideas to another level. Therefore, possible realization of proposed design using commercially available Texas Instruments OTA IC, CA3080 (pin configuration of IC CA3080 is shown in **Figure 21**) is explored and given in **Figure 22**. The real time experimental set up of mixed mode APF in VM is shown in **Figure 23**. The circuit is designed at pole frequency of 8.359 kHz with values of passive components as R = 19.55 kΩ, C = 1 nF and bias currents, $I_{B1} = I_{B2} = 7.95$ µA. The power supplies are taken as ±6 V. The experimental transient response of the presented circuit is shown in **Figure 24** that again confirms 90 ° phase shift between input and output at pole frequency as expected.

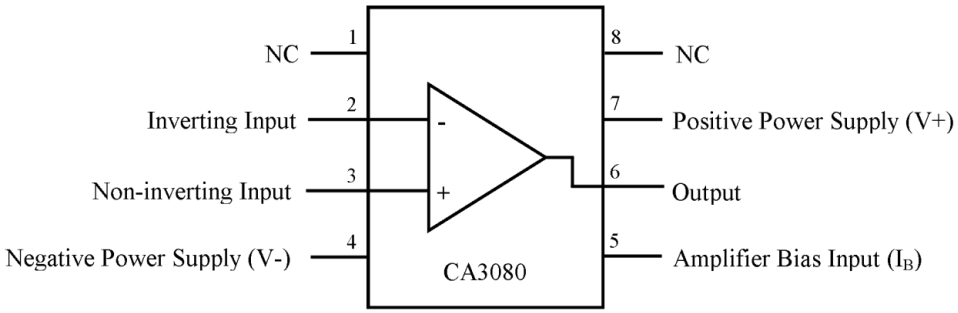

Figure 21 Pin configuration of commercially available OTA, CA3080.

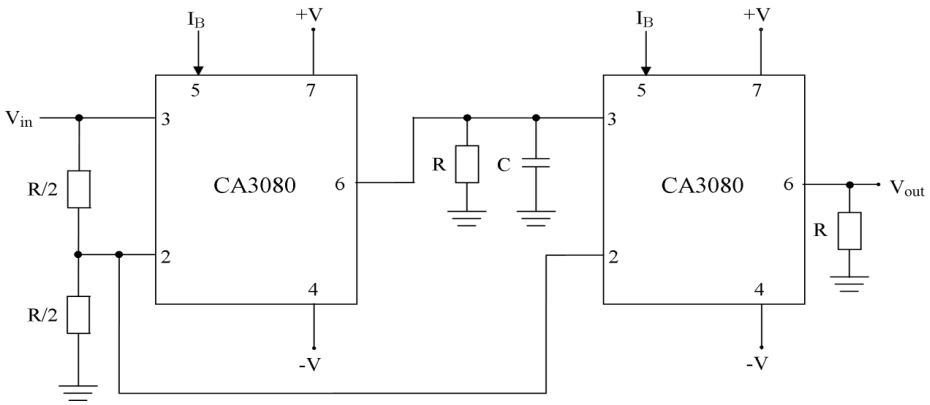

Figure 22 Experimental realization of mixed mode APF in VM using commercially OTA IC, CA3080.

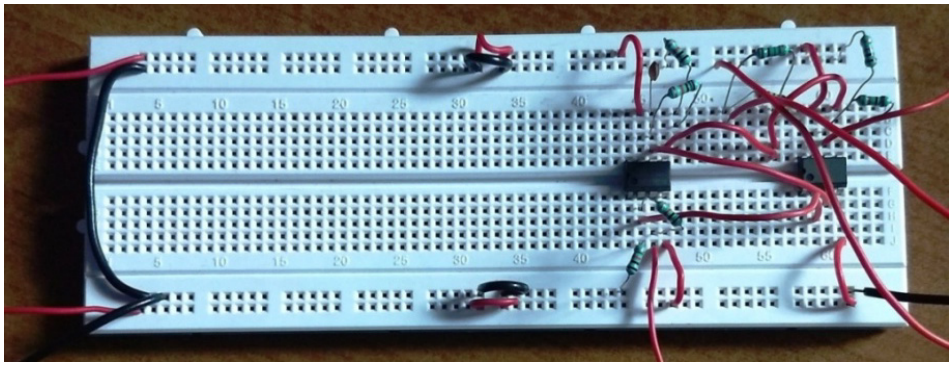

Figure 23 Experimental setup of mixed mode APF in VM.

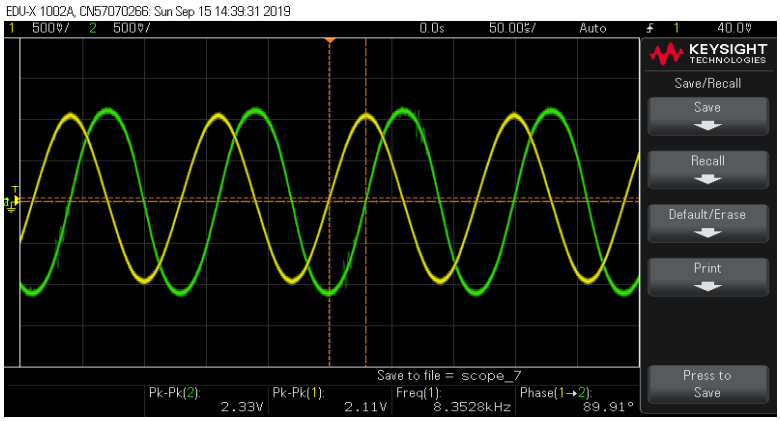

Figure 24 Experimental transient response of **Figure 23** at pole frequency.

Conclusions

In this paper, a new structure of first order mixed mode MOS-C APF is presented that can operate in all 4 possible mode of operation. Employment of only 1 passive component increases the beauty of the proposed design. The presented idea also enjoys a very substantial attribute of electronic tunability. The proposed circuit is found to be better in terms of active and passive component count, transistors count, load sensitivity, THD, appropriate input and output impedances, use of grounded capacitor, resistorless realization, good operating frequency, low power, low voltage and also have flexibility to operate in all 4 possible modes. The detailed study including possible focus on non-ideal aspects is incorporated to exploit real time performance of novel frequency selective structure. The presented theoretical validations are confirmed through PSPICE simulation results. In addition, the practicability and feasibility aspects are covered by exploring experimental realization of proposed APF using commercially available ICs. The presented first order filter may find suitable and useful applications in the various areas of signal processing.

References

[1] R Senani, DR Bhaskar and AK Singh. *Current conveyors: Variants, applications, and hardware implementations.* Springer International Publication, Cham, Switzerland, 2015, p. 1-574.

[2] RL Geiger and E Sanchez-Sinencio. Active filter design using operational transconductance amplifiers: A tutorial. *IEEE Circ. Dev. Mag.* 1985; **1**, 20-32.

[3] IA Khan and MT Ahmed. Electronically tunable first order OTA-capacitor filter sections. *Int. J. Electron*. 1986; **61**, 233-7.

[4] NA Shah and SN Ahmad. Electronically tunable OTA-based all-pass circuit. *Int. J. Electron. Theor. Exp*. 1990; **68**, 963-6.

[5] MT Abuelma'atti and U Baroudi. A programmable phase shifter for sinusoidal signals. *Active Passive Electron. Compon*. 1998; **21**, 107-12.

[6] BM Al-Hashimi, F Dudek and Y Sun. Current-mode delay equalizer design using multiple output OTAs. *Analog Integrated Circ. Signal Process.* 2000; **24**, 163-9.
[7] S Minaei and O Cicekoglu. New current-mode integrator and all-pass section without external passive elements and their application to design a dual-mode quadrature oscillator. *Frequenz* 2003; **57**, 19-24.
[8] AÜ Keskin, K Pal and E Hancioglu. Resistorless first-order all-pass filter with electronic tuning. *AEU Int. J. Electron. Comm.* 2008; **62**, 304-6.
[9] B Metin, K Pal, S Minaei and O Cicekoglu. Trade-offs in the OTA-based analog filter design. *Analog Integrated Circ. Signal Process.* 2009; **60**, 205-13.
[10] N Herencsar, J Koton and K Vrba. A new electronically tunable voltage-mode active-C phase shifter using UVC and OTA. *IEICE Electron. Exp*. 2009; **6**, 1212-8.
[11] C Psychalinos and K Pal. A novel all-pass current-mode filter realized using a minimum number of single output OTAs. *Frequenz* 2010; **64**, 30-2.
[12] T Tsukutani, H Tsunetsugu, Y Sumi and N Yabuki. Electronically tunable first-order all-pass circuit employing DVCC and OTA. *Int. J. Electron*. 2010; **97**, 285-93.
[13] D Biolek and V Biolkova. First-order voltage-mode allpass filter employing one active element and one grounded capacitor. *Analog Integrated Circ. Signal Process*. 2010; **65**, 123-9.
[14] SZ Iqbal, C Psychalinos and N Parveen. First-order allpass filter using multi-input OTA. *Int. J. Electron*. 2013; **100**, 1373-82.
[15] R Sotner, J Jerabek, N Herencsar, R Prokop, K Vrba and T Dostal. Resistor-less first-order filter design with electronical reconfiguration of its transfer function. *In*: Proceedings of the 24th International Conference Radioelektronika, Bratislava, Slovakia. **2014**, p. 1-4.
[16] A Jantakun and W Jaikla. Active-only current-mode first-order allpass filter and its application in quadrature oscillator. *Indian J. Pure Appl. Phys.* 2015; **53**, 557-63.
[17] W Jaikla, P Talabthong, S Siripongdee, P Supavarasuwat, P Suwanjan and A Chaichana. Electronically controlled voltage mode first order multifunction filter using low-voltage low-power bulk-driven OTAs. *Microelectron. J*. 2019; **91**, 22-35.
[18] G Singh. CMOS realization of VDVTA and OTA based fully electronically tunable first order all pass filter with optimum linearity at low supply voltage ±0.85 V. *Circ. Syst*. 2020; **11**, 39-49.
[19] M Kumngern, J Chanwutitum and K Dejhan. Electronically tunable voltage-mode all-pass filter using simple CMOS OTAs. *In*: Proceedings of the International Symposium on Communications and Information Technologies (ISCIT2008), Vientiane, Laos. 2008, p. 1-5.
[20] BP Das, N Watson and Y Liu. Wide tunable all pass filter using OTA as active component. *In*: Proceedings of the International Conference on Signals and Electronic Systems (ICSES2010), Gliwice, Poland. 2010, p. 379-82.
[21] T Tsukutani, H Tsunetsugu, Y Sumi and N Yabuki. Electronically tunable first order all-pass sections using OTAs. *In*: Proceedings of the International Conference on Computer Applications and Industrial Electronics (ICCAIE 2010), Kuala Lumpur, Malaysia. 2010, p. 548-51.
[22] M Kumngern. Realization of electronically tunable first-order allpass filter using single-ended OTAs. *In*: Proceedings of the IEEE Symposium on Industrial Electronics and Applications, Bandung, Indonesia. 2012, p. 100-3.
[23] R Sotner, J Jerabek, N Herencsar, R Prokop, K Vrba and T Dostal. Resistor-less first-order filter design with electronical reconfiguration of its transfer function. *In*: Proceedings of the 24th International Conference on Radioelektronika, Bratislava, Slovakia. 2014, p. 63-6.
[24] J Petrzela and R Sotner. Systematic design procedure towards reconfigurable first-order filters. *In*: Proceedings of the 24th International Conference on Radioelektronika, Bratislava, Slovakia. 2014, p. 237-40.
[25] T Zak, R Sotner, J Jerabek, K Vrba and T Dostal. Reconfigurable first-order filter operating with non-ideal parameters of active elements. *In*: Proceedings of the International Conference on Applied Electronics, Pilsen, Czech Republic. 2015, p. 293-6.
[26] M Gupta, TS Arora and SN Gupta. A novel current-mode and voltage-mode all pass filter employing operational transconductance amplifier. *In*: Proceedings of the 1st IEEE International Conference on Power Electronics, Intelligent Control and Energy Systems (ICPEICES), New Delhi, India. 2016.
[27] R Verma, N Pandey and R Pandey. Electronically tunable fractional order all pass filter. *IOP Conf. Ser. Mater. Sci. Eng.* 2017; **225**, 012229.
[28] M Bhanja and B Ray. A hierarchical and programmable OTA-C filter. *In*: Proceedings of the IEEE Computer Society Annual Symposium on VLSI (ISVLSI 2017), Bochum, Germany. 2017, p. 513-8.

[29] P Prommee, K Angkeaw, J Chanwutitum and K Dejhan. Dual input all-pass networks using MO-OTA and its application. *In*: Proceedings of the ECTI-CON 2007, Chiang Rai, Thailand. 2007, p. 129-32.
[30] E Saising and P Prommee. Fully tunable all-pass filter using OTA and its application. *In*: Proceedings of the 39th International Conference on Telecommunications and Signal Processing (TSP), Vienna, Austria. 2016, p. 287-90.
[31] DV Kamat, PA Mohan and KG Prabhu. Novel first-order and second-order current mode filters using dual-output OTAs and grounded capacitors. *In*: Proceedings of the TENCON 2008 IEEE Region 10 Conference, Hyderabad, India. 2008.
[32] DV Kamat, PA Mohan and KG Prabhu. Novel first-order and second-order current-mode filters using multiple-output operational transconductance amplifiers. *Circ. Syst. Signal Process.* 2010; **29**, 553-76.
[33] T Prommas, W Jaikla, P Suwanjan and P Silapan. Design of electronically tunable first order allpass filter using OTAs with gain controllability. *In*: Proceedings of the 13th International Symposium on Communications and Information Technologies (ISCIT), Surat Thani, Thailand. 2013, p. 350-3.
[34] Jitender, J Mohan and B Chaturved. CMOS realizable and highly cascadable structures of first-order all-pass filters. *Walailak J. Sci. Tech.* 2021; **18**, 21451-19.
[35] A Chaichana, S Siripongdee and W Jaikla. Electronically adjustable voltage-mode first-order allpass filter using single commercially available IC. *IOP Conf. Ser. Mater. Sci. Eng.* 2019; **559**, 012009.
[36] J Mohan, B Chaturvedi and A Kumar. New CMOS realizable all-pass frequency selective structures. *J. Circ. Syst. Comput.* 2021; **30**, 2150268.
[37] M Faseehuddin, J Sampe, S Shireen and SH Ali. Minimum component all pass filters using a new versatile active element. *J. Circ. Syst. Comput.* 2020; **29**, 2050078.
[38] R Senani, DR Bhaskar and P Kumar. Two-CFOA-grounded-capacitor first-order all-pass filter configurations with ideally infinite input impedance. *AEU Int. J. Electron. Comm.* 2021; **137**, 153742.
[39] Jitender, J Mohan and B Chaturvedi. Realization of generalized current-mode multifunction filter. *J. Circ. Syst. Comput.* 2021; **30**, 2150211.
[40] PE Allen and DR Holberg. *CMOS analog circuit design*. Oxford University Press, New York, 2002.
[41] Z Wang. 2-MOSFET transresistor with extremely low distortion for output reaching supply voltages. *Electron. Lett*. 1990; **26**, 951-2.